

Self-passivating tungsten alloys for first wall applications

Christian Linsmeier

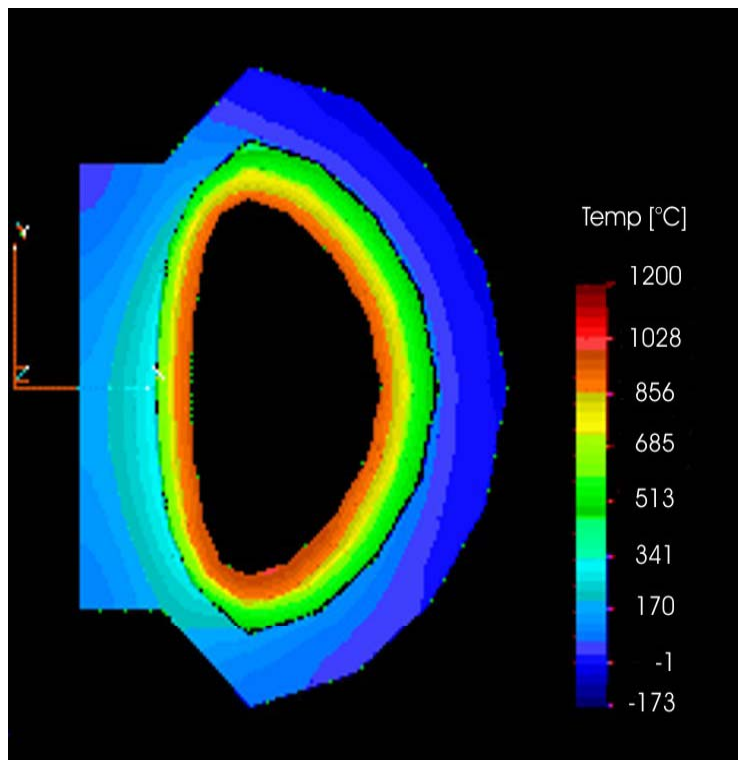
**Freimut Koch, Christian Lenser, Stefan Lindig, Marcin Rasinski,
Martin Balden, Annegret Brendel**

*Max-Planck-Institut für Plasmaphysik
Garching b. München, Germany*

- Applications: ITER and DEMO
- Self-passivation mechanism
- Quaternary alloys
- W-Si-Cr bulk materials

Accidental loss of coolant in reactor

Power plant conceptual study



Temperature profile in PPCS Model A, 10 days after accident with a total loss of all coolant.

[Final Report of the European Fusion Power Plant Conceptual Study, 2004]

- Accidental loss of coolant: peak temperatures of first wall up to 1200 °C due to nuclear afterheat
- Additional air ingress: formation of highly volatile WO_3 (Re, Os)
- Evaporation rate: order of 10 -100 kg/h at $>1000^\circ\text{C}$ in a reactor (1000 m² surface)
→ large fraction of radioactive WO_3 may leave hot vessel



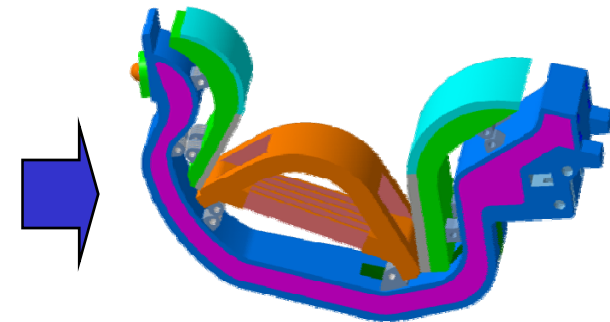
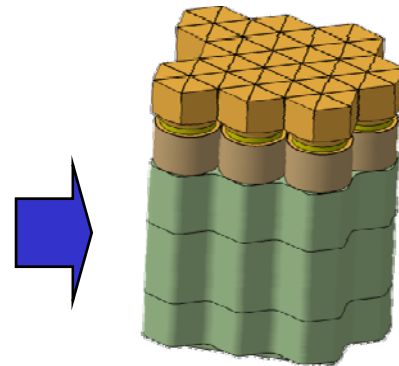
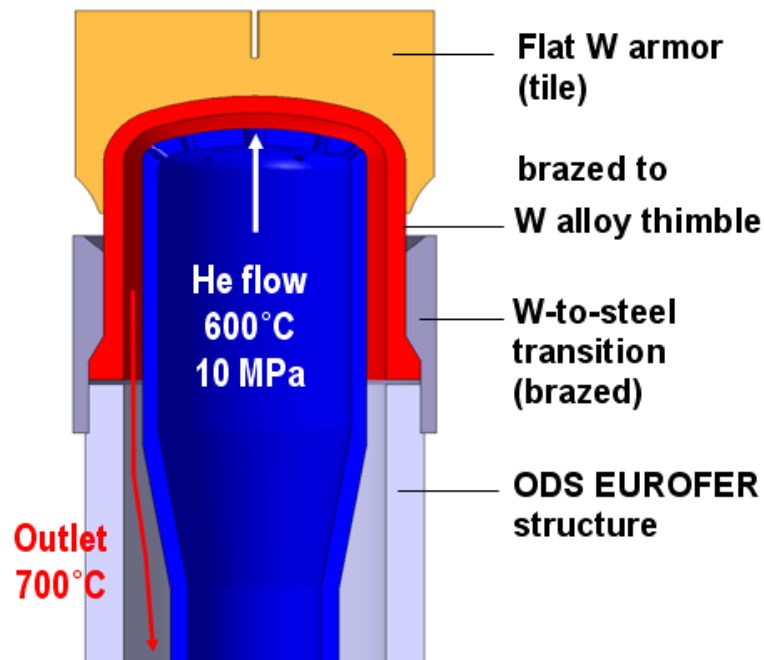
Development of self-passivating tungsten alloys

He-cooled divertor modular design for DEMO (KIT)



He-cooled multi-jet (HEMJ) concept

P. Norajitra, KIT



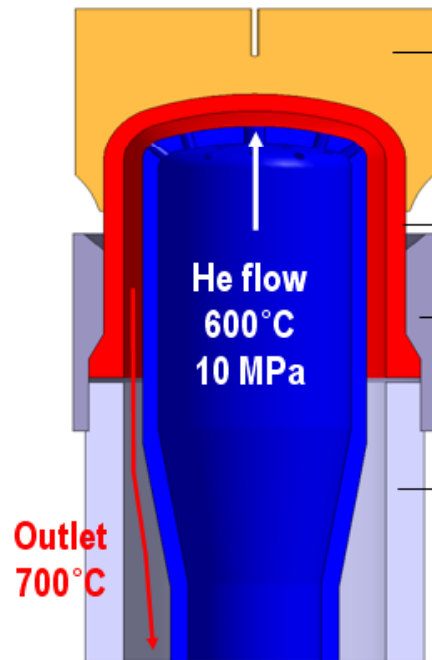
Test divertor module
to be proposed for
testing in ITER

Goal: $\geq 10 \text{ MW/m}^2$,
100-1000 load cycles

He-cooled divertor modular design for DEMO (KIT)



He-cooled multi-jet (HEMJ) concept



Goal: $\geq 10 \text{ MW/m}^2$,
100-1000 load cycles

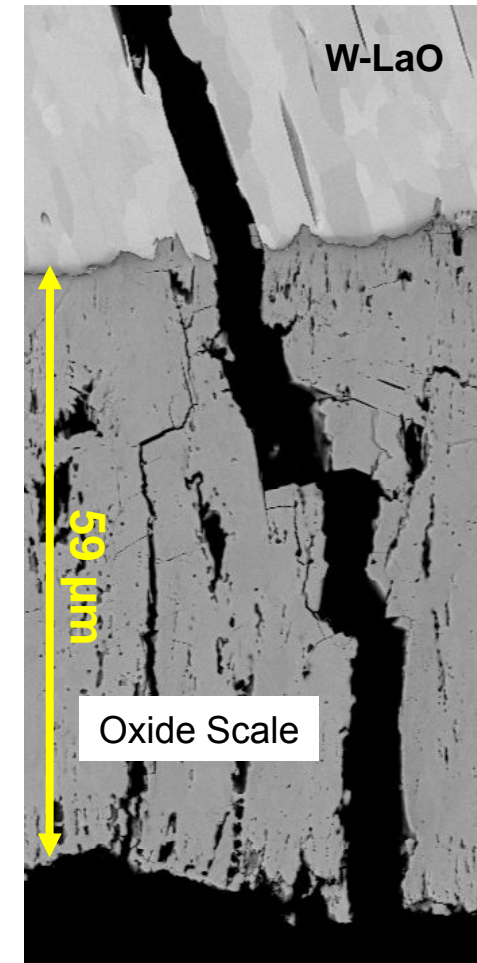
Post-examination after
HHF tests at FZJ
(90 load cycles at
 9 MW/m^2):

- Formation of thick oxide scale
- Crack propagation



Application for self-passivating tungsten alloys

P. Norajitra, KIT



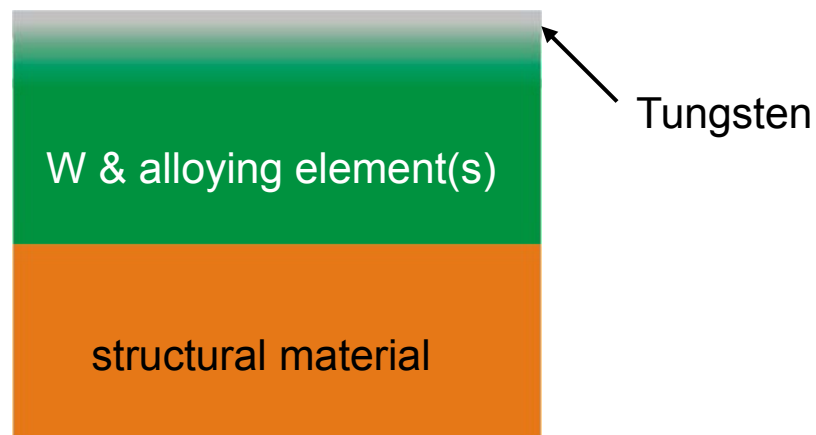
HHF tests at $10 \mu\text{m}$
Efremov (test range
 $5\text{-}13 \text{ MW/m}^2$)

Self passivating tungsten-based alloys:

Surface composition automatically adjusts to the requested property

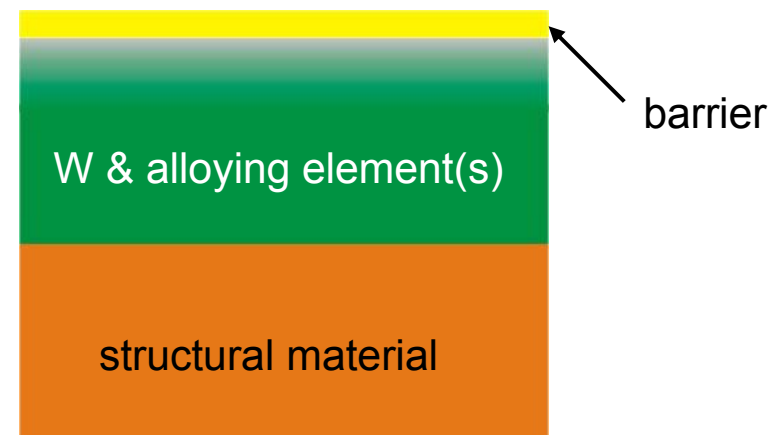
Normal operation (600°C):

Formation of tungsten surface by depletion of alloying element(s) due to preferential sputtering



Accidental conditions:

(air ingress, up to 1200 °C)
Formation of protective barrier layer

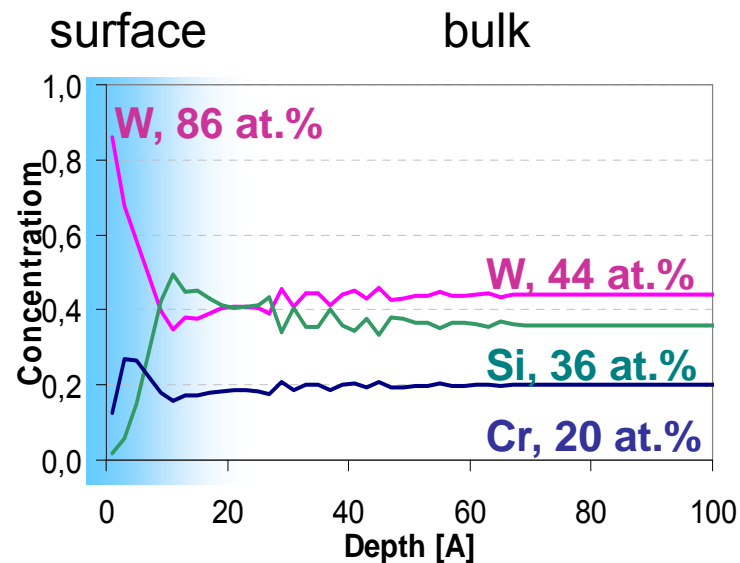


Self passivating tungsten-based alloys:

Surface composition automatically adjusts to the requested property

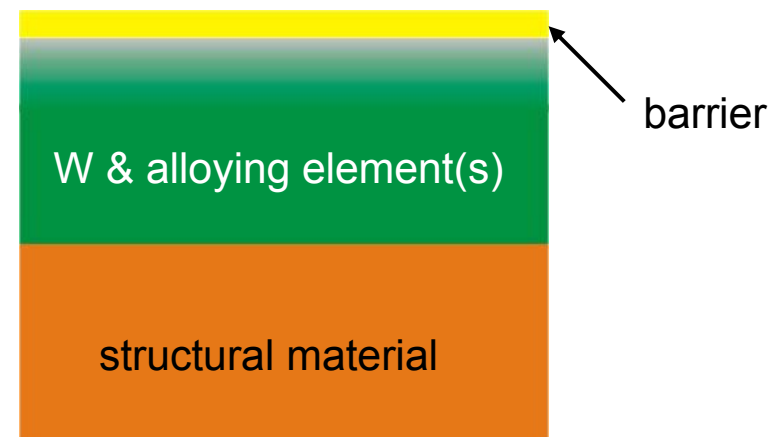
Normal operation (600°C):

TRIDYN numerical simulation of sputter erosion of W-Si-Cr alloy (D ions, 30 eV, fluence $10^{18}/\text{cm}^2$)



Accidental conditions:

(air ingress, up to 1200 °C)
Formation of protective barrier layer

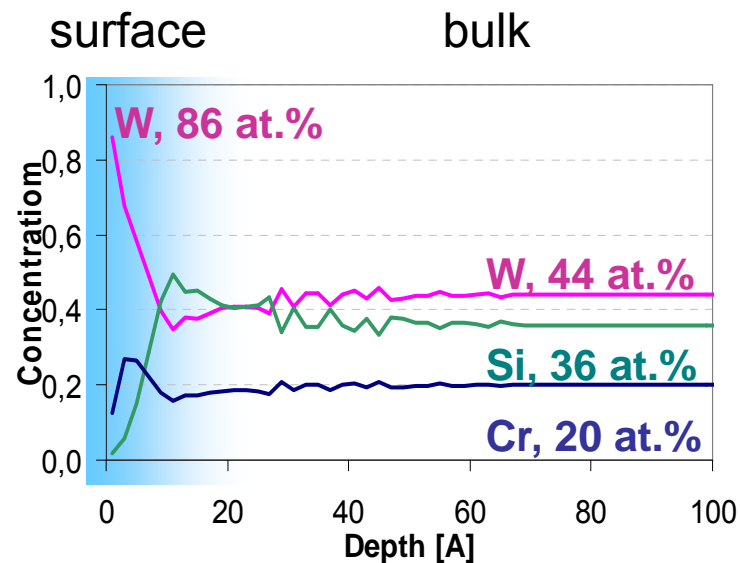


Self passivating tungsten-based alloys:

Surface composition automatically adjusts to the requested property

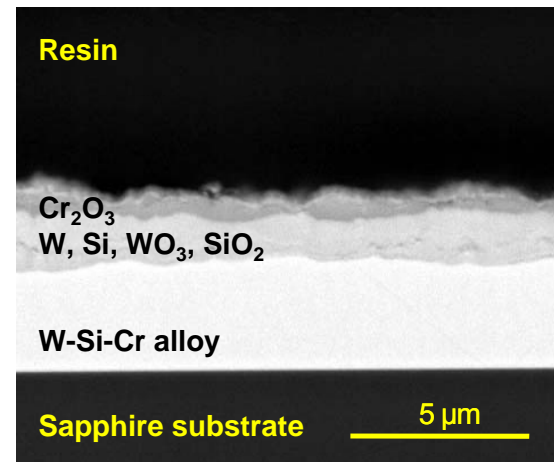
Normal operation (600°C):

TRIDYN numerical simulation of sputter erosion of W-Si-Cr alloy (D ions, 30 eV, fluence $10^{18}/\text{cm}^2$)



Accidental conditions:

Cross section of sputter deposited W-Si-Cr film after oxidation at 1000°C for 1h



Addition of reactive elements to W-Si-Cr to improve oxide film formation and adherence

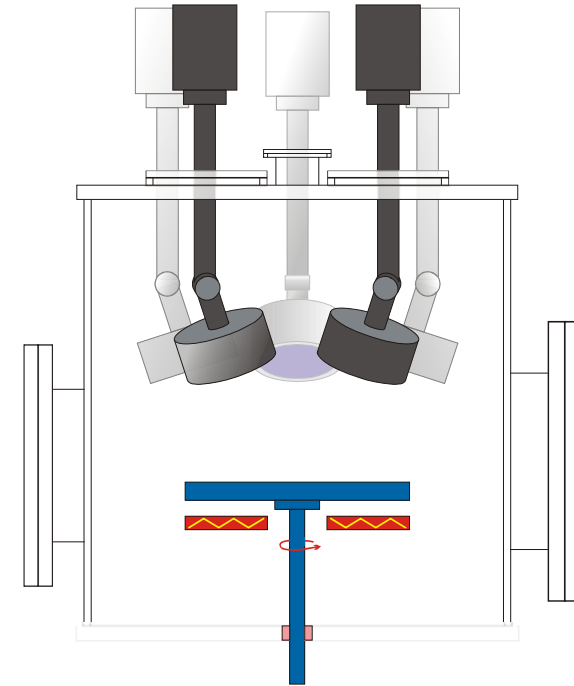
Co-deposition by Magnetron sputtering

- Film thickness $\sim 4\mu\text{m}$
- SiO_2 and Al_2O_3 substrates used for oxidation

Investigated systems

- W-Si-Cr-Zr
- W-Si-Cr-Y

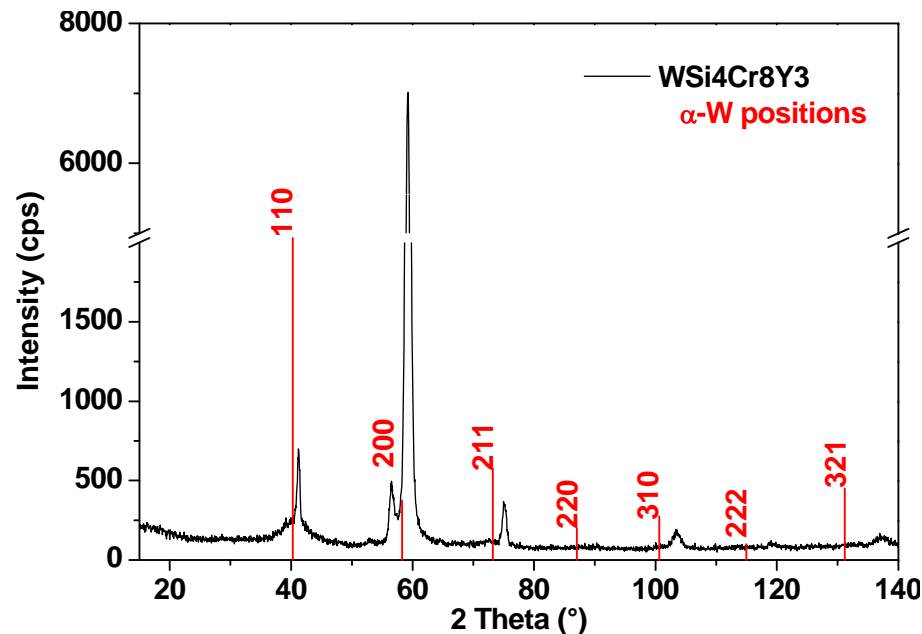
(different concentrations)



Schematic view of deposition facility

XRD analysis: alloys as deposited

Peak shift due to Lattice Distortion

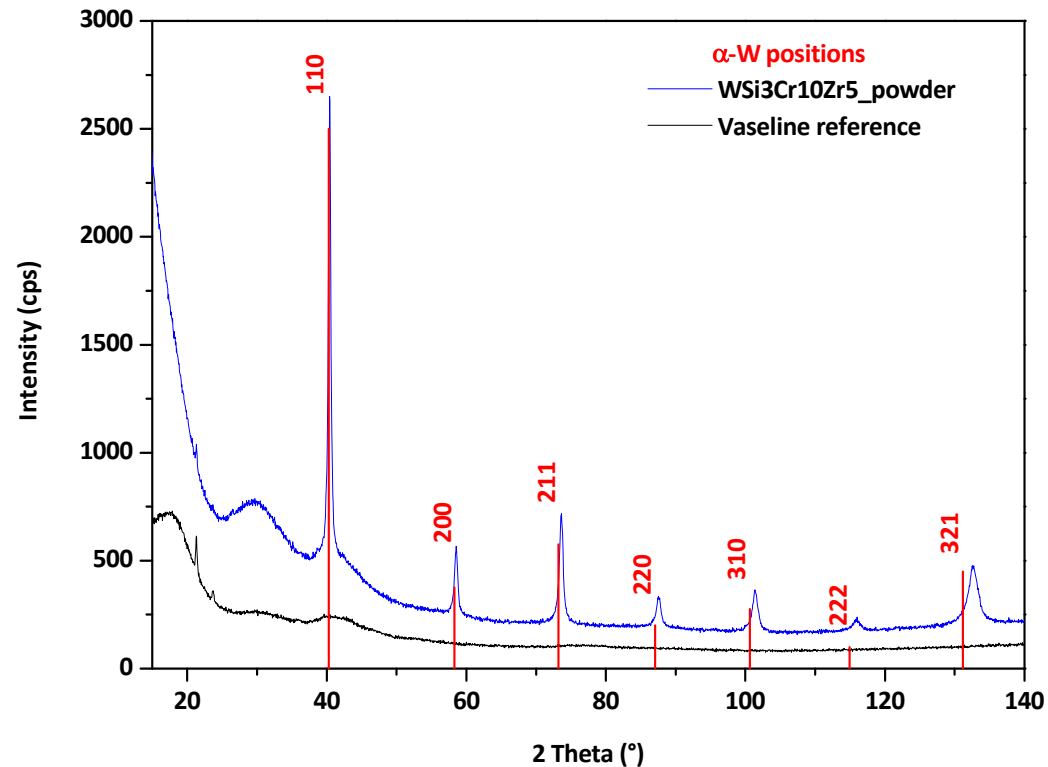


d	2θ	h	k	l
Angström	°			
2,2976	39.177	1	1	0
2,1922	41.1438	1	1	0
1,5567	59.3162	2	0	0
1,3043	72.3989	2	1	1
1,2668	74.8987	2	1	1
0,9823	103.2851	3	1	0
0,8283	136.8753	3	2	1

- Fifth order polynomial by Gust et al. used to calculate W concentration in assumed binary W-Cr lattice
- $c(\text{Cr}) = 27.5 \text{ at-\%}$ from peak shift; $c(\text{Cr}) = 29.2 \text{ at-\%}$ from RBS

Gust, W.; Predel, B.; Roll, U.: Journal of the Less-Common Metals, 69, pp. 331-353, 1980

XRD analysis: annealed alloys

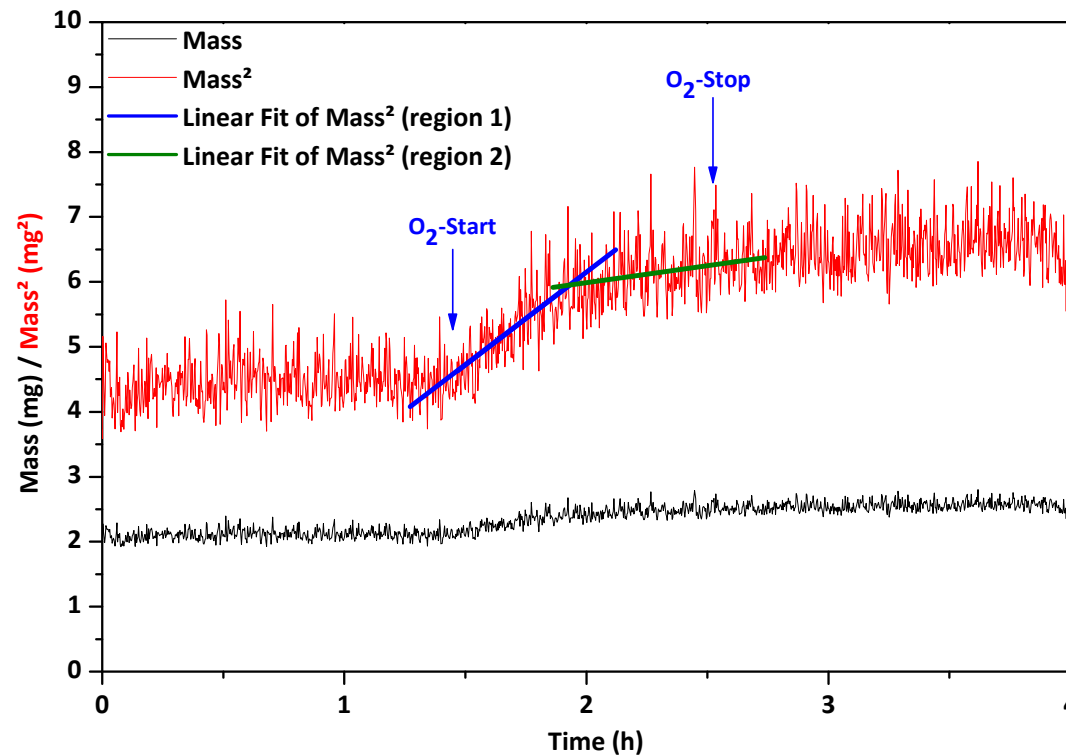


WSi₃Cr₁₀Zr₅ powder

(annealed at 1000 °C under Ar)

- $c(\text{Cr}) = 24 \text{ at-}\%$ after deposition (RBS); $c(\text{Cr}) = 6.75 \text{ at-}\%$ after annealing
- Thermodynamic equilibrium: $c(\text{Cr}) = 7 \text{ at-}\%$ (Gust et al.)
- Cr precipitates from the binary lattice

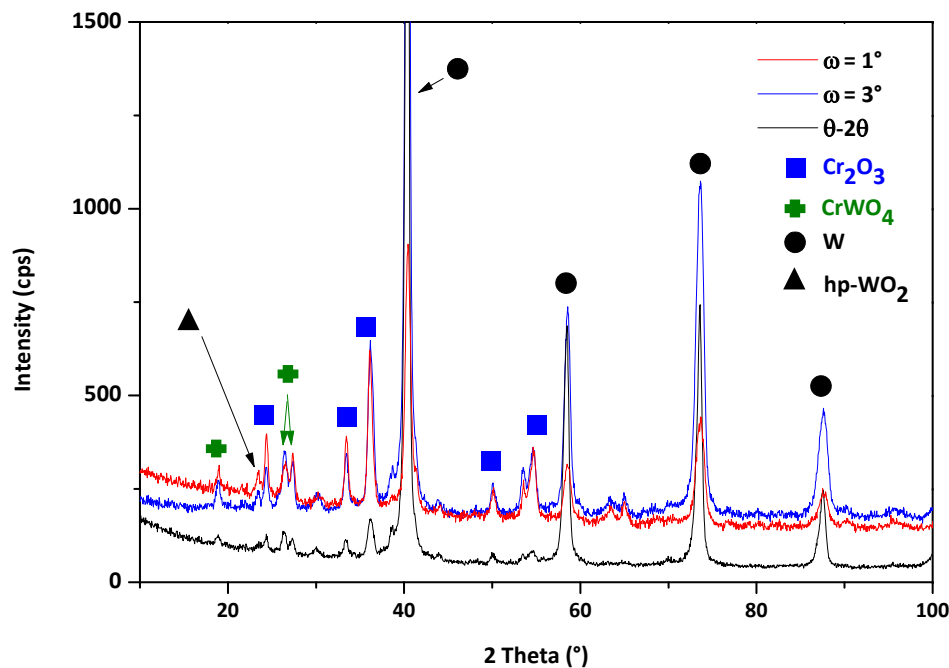
Oxidation of W-Si4-Cr8-Y3 at 1000°C for 1 hours



- Heating under inert gas flow
- Start of oxygen at stable temperature

- Parabolic oxidation rates: $(\Delta m)^2 = k t$: → Diffusion-governed process
- Two oxidation rates discernible

XRD analysis: oxidized alloys



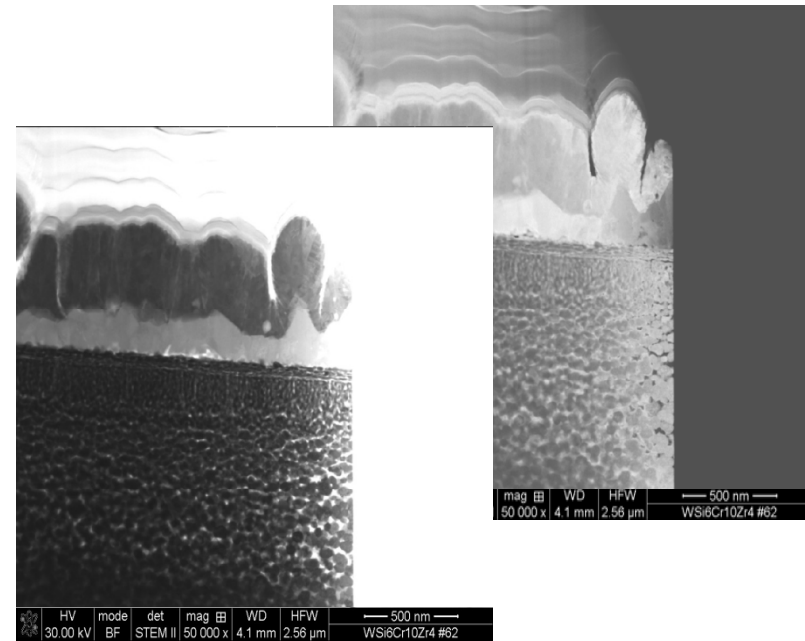
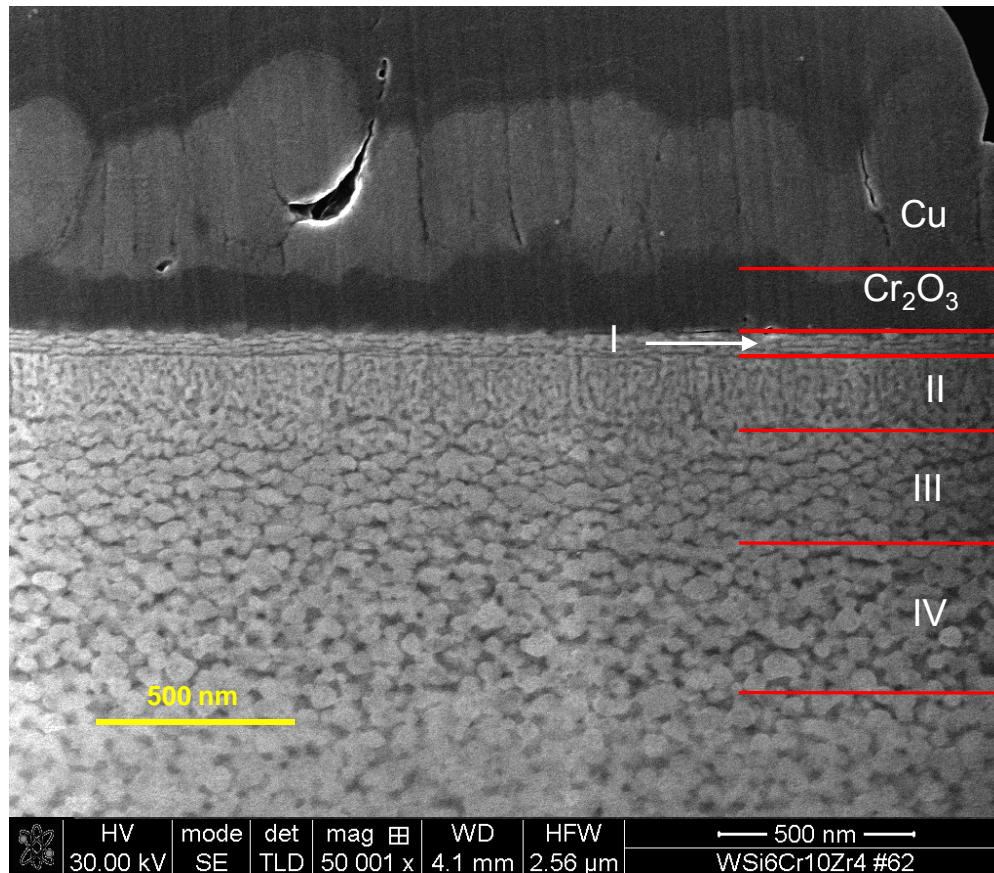
WSi₃Cr₁₀Zr₅ (oxidized 1h at 1000 °C)

Phases identified by XRD			
Ox. temp.	600°C	800°C	1000°C
Ox. time	48 h	4 h	1 h
	Cr ₂ O ₃	Cr ₂ O ₃	Cr ₂ O ₃
	CrWO ₄	CrWO ₄	CrWO ₄
	W	W	W
	WO ₂	WO ₂	
	hp-WO ₂	hp-WO ₂	hp-WO ₂
	ZrSiO ₄		

→ no volatile WO₃ formed!

Microstructure of oxidized alloys

WSi3Cr10Zr5:

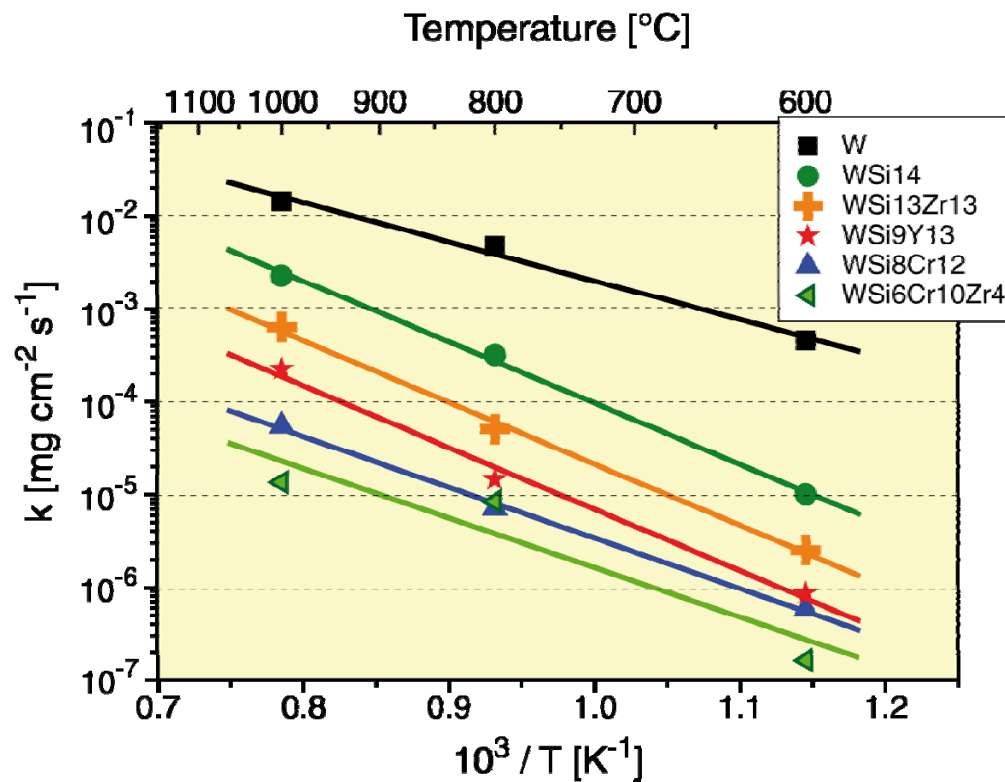


- Dense Cr₂O₃ barrier scale
- Cr is main diffusing species
- Mixed oxide zone(s)
- Cr depletion zone with voids
- No formation of WO₃

SEM of cross section (FIB), 1000°C, 1h

Comparison of oxidation results

Arrhenius plot of oxidation rates of tungsten and tungsten alloys



Alloy	W	Si	Cr	Zr
WSi8Cr12	46	30	24	-
WSi3Cr10Zr5	56	13	24	7

Composition in at.%

Oxidation rate (k) has been calculated from weight increase versus time, linear fit.

Linear oxidation rates of W-Si-Cr & quaternary alloys comparable.
 Quaternary alloys show distinct parabolic oxidation behavior at reduced level of alloying elements.

- **Quaternary alloys** show better passivation behavior than ternary while **containing more W**
- Active elements (Y/Zr) do not form oxide layers, but **improve oxide scale adhesion**
- Surface oxide consists of **Cr₂O₃**
- Oxide phases formed are Cr₂O₃, WCrO₄, WO₂ (2 modifications), ZrSiO₄ (600°C), but **no WO₃ → passivation successful**
- **Two step-oxidation**: switch in oxidation mechanism during oxidation
- Different oxidation **mechanisms** at different **temperatures**
- Restructuring induced by the **precipitation of Cr from the W lattice**

Ternary alloys: bulk samples

Samples:

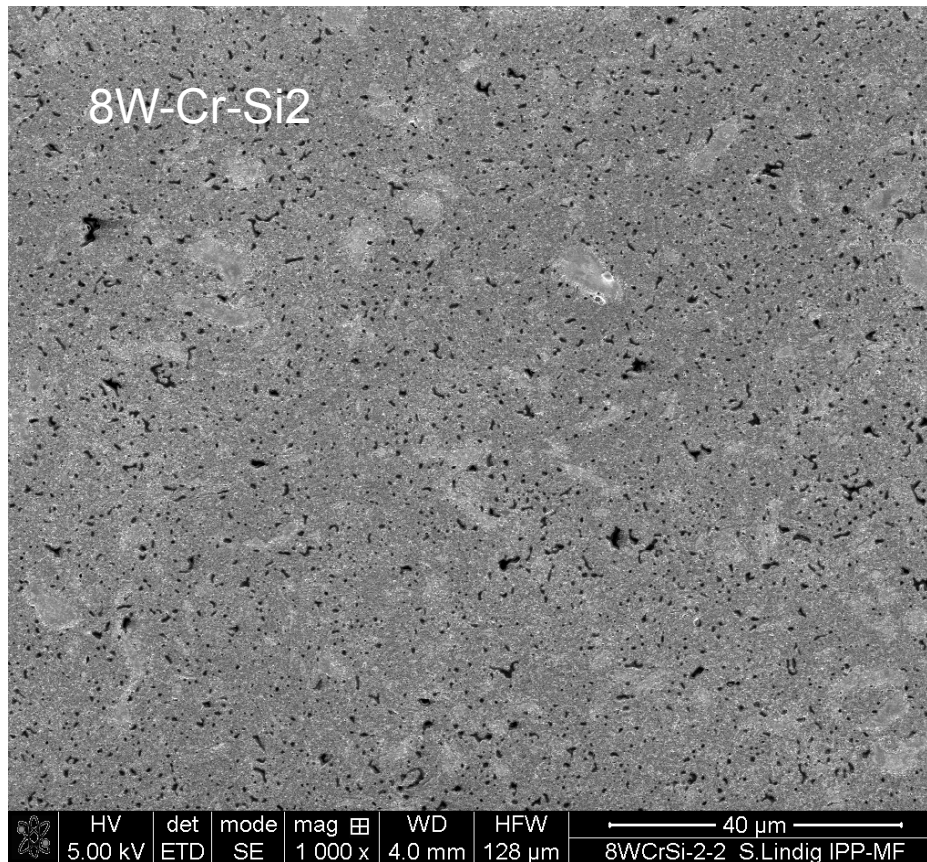
8W-Cr-Si₂ and 8W-Cr-Si₄

nominal composition: **W Si10 Cr10**

Investigated properties:

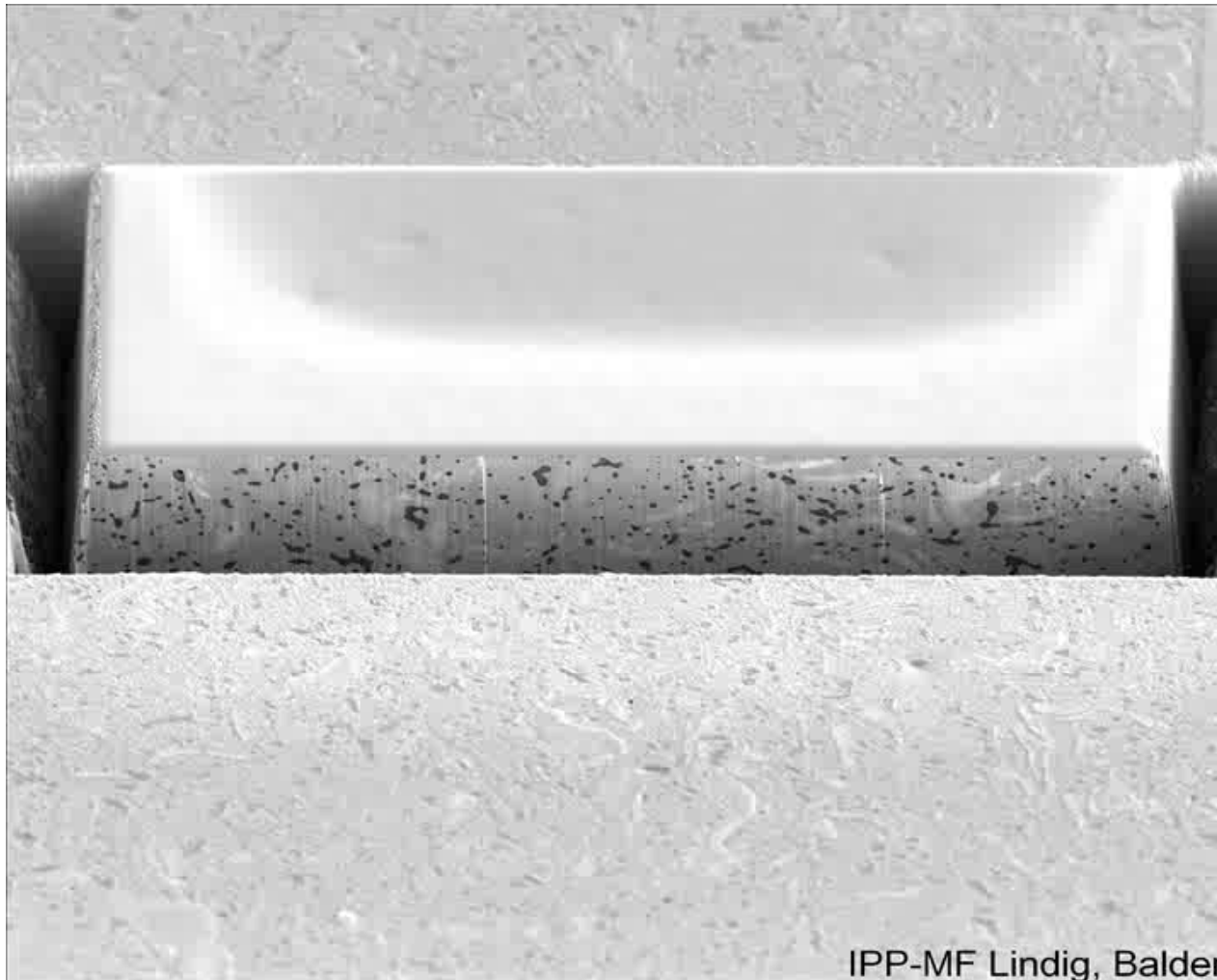
- morphology
- element distribution
- thermal diffusivity
- hardness / Young's modulus
- oxidation behavior

Collaboration with CEIT / San Sebastián



- W phases dominate: gray areas
- pure W (bright) to W alloys
- small oxidic precipitates (no W!)

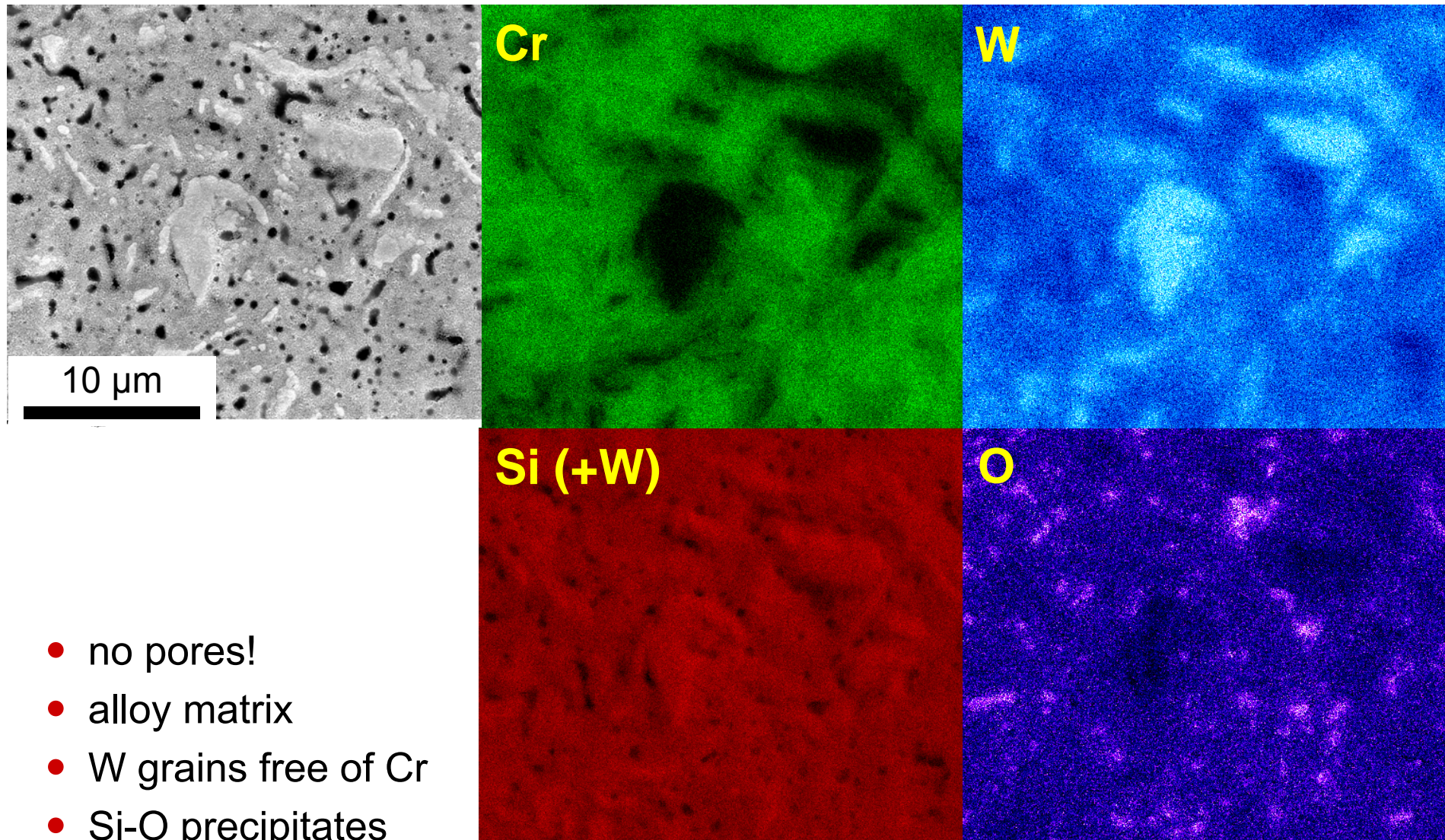
3D analysis: Focused ion beam



width of cut: $\sim 75 \mu\text{m}$

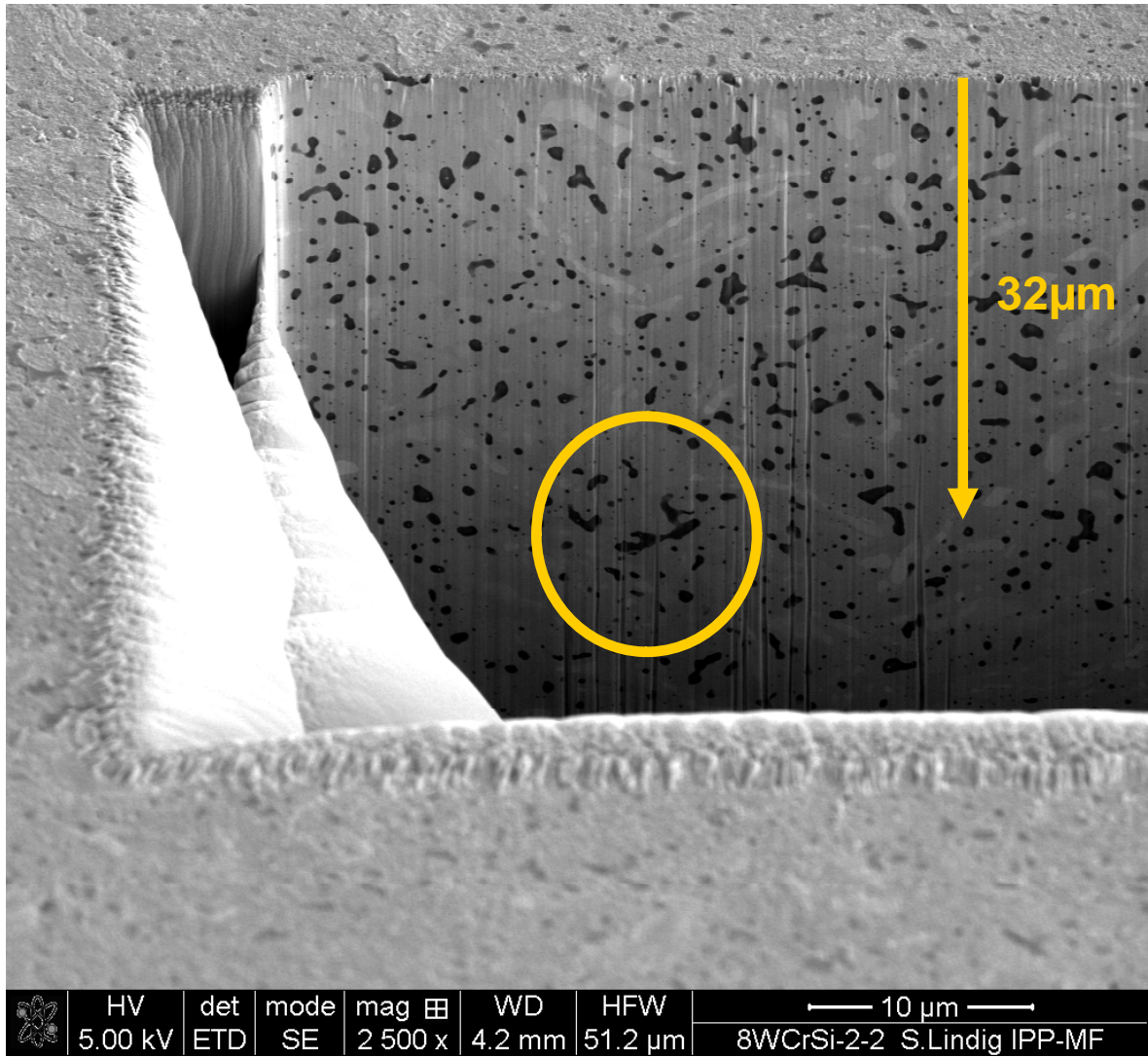
- 3D morphology identical to surface

2D element distribution

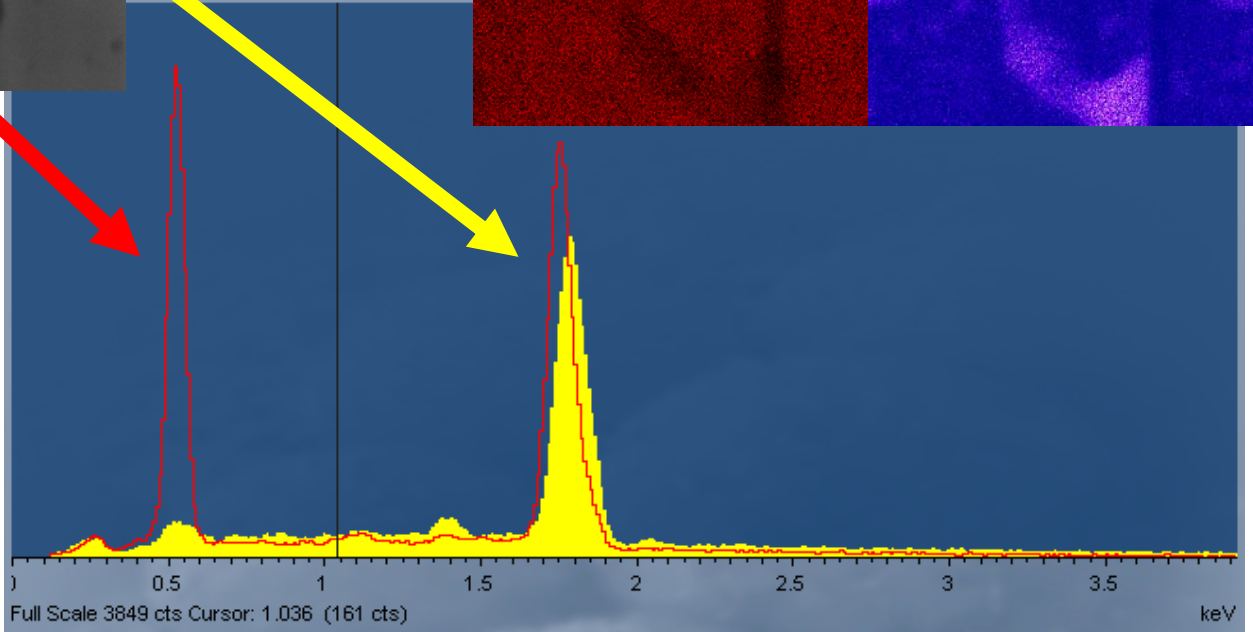
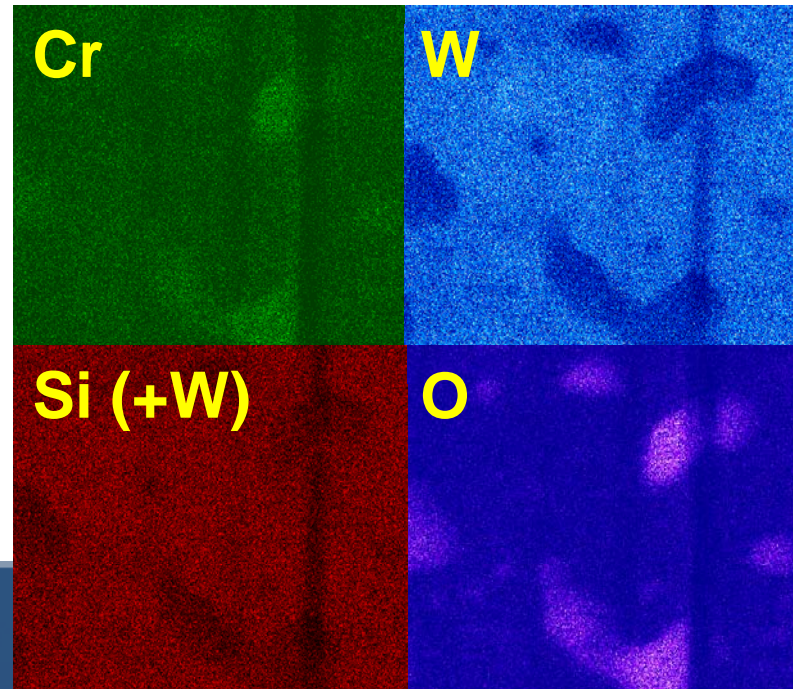
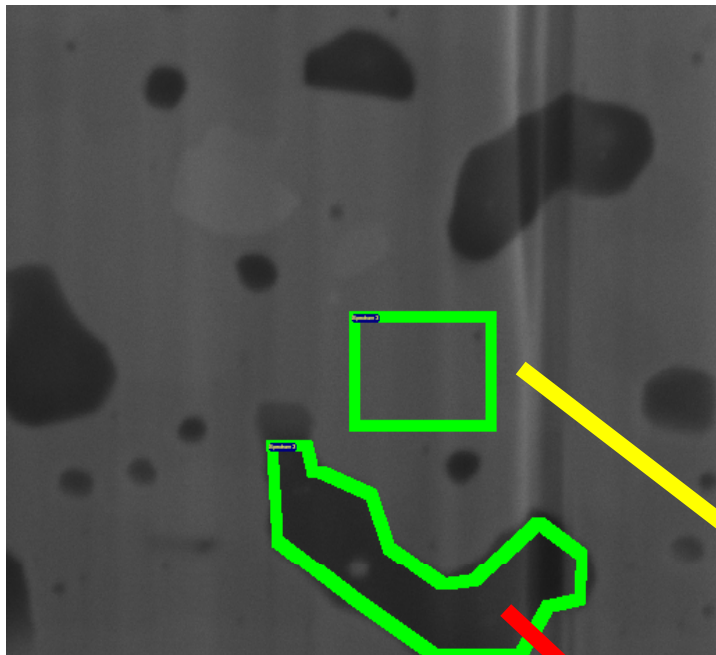


- no pores!
- alloy matrix
- W grains free of Cr
- Si-O precipitates

Cross-section 8W-Cr-Si2

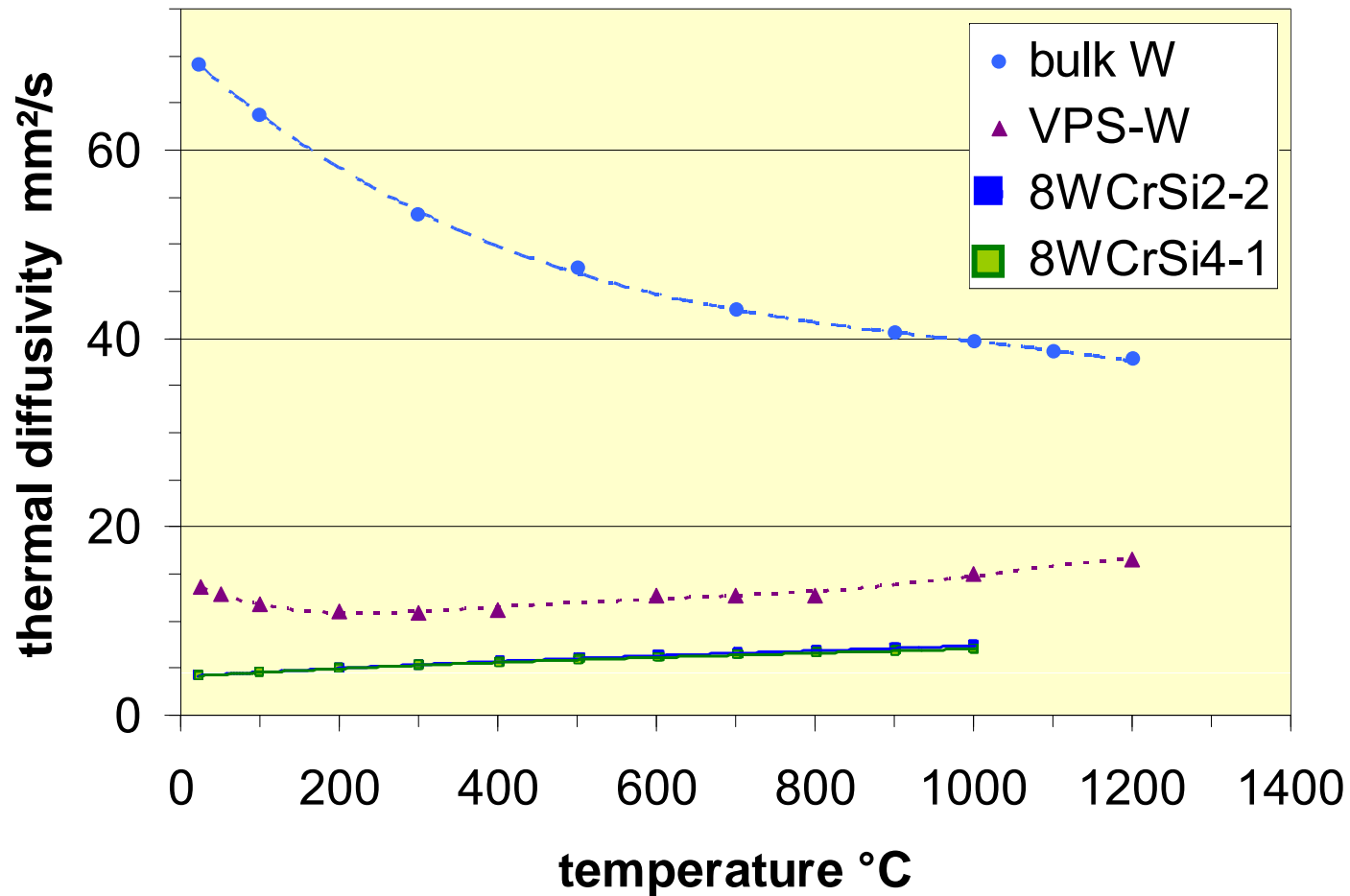


3D element distribution



- no pores!
- alloy matrix
- W grains free of Cr
- Si-O precipitates

Thermal diffusivity

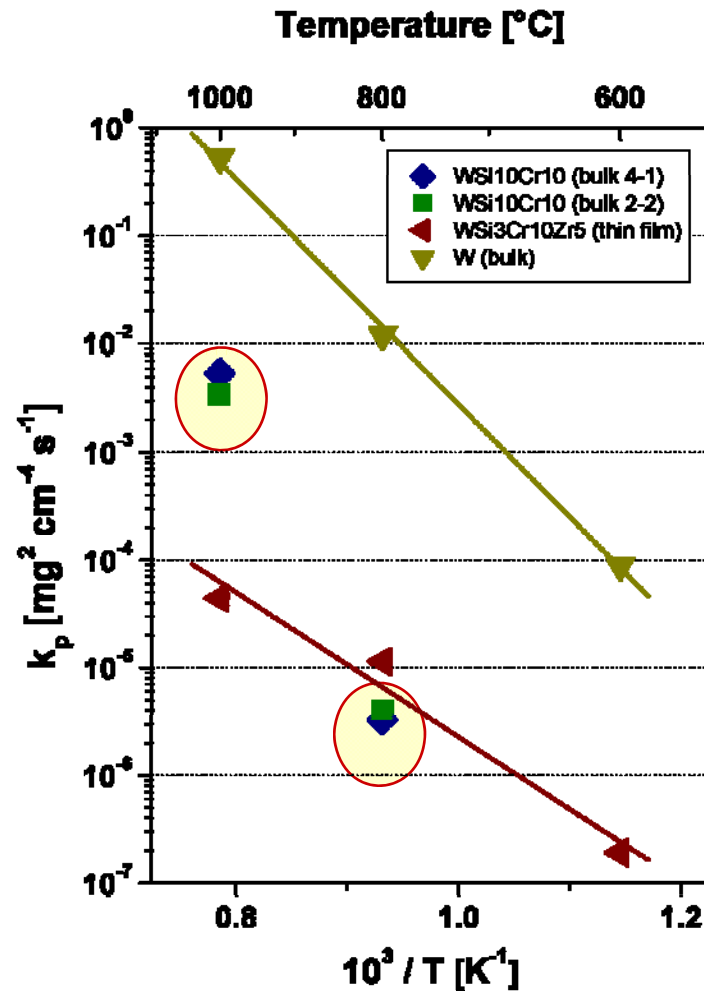


- constant thermal diffusivity
- 50% value of VPS-W

Nanoindenter: micro-hardness, Young's modulus

	Micro-hardness [GPa]	Young's modulus [GPa]
alloys:		
8W-Cr-Si₂	15.6	320
8W-Cr-Si₄	15.5	321
comparison:		
W_f/W (fiber)	9.1—9.8	480—535
W_f/W (CVD-W)	7.5—8.1	455—530
(dense bulk W)		410)

Oxidation rates for bulk W Si10 Cr10



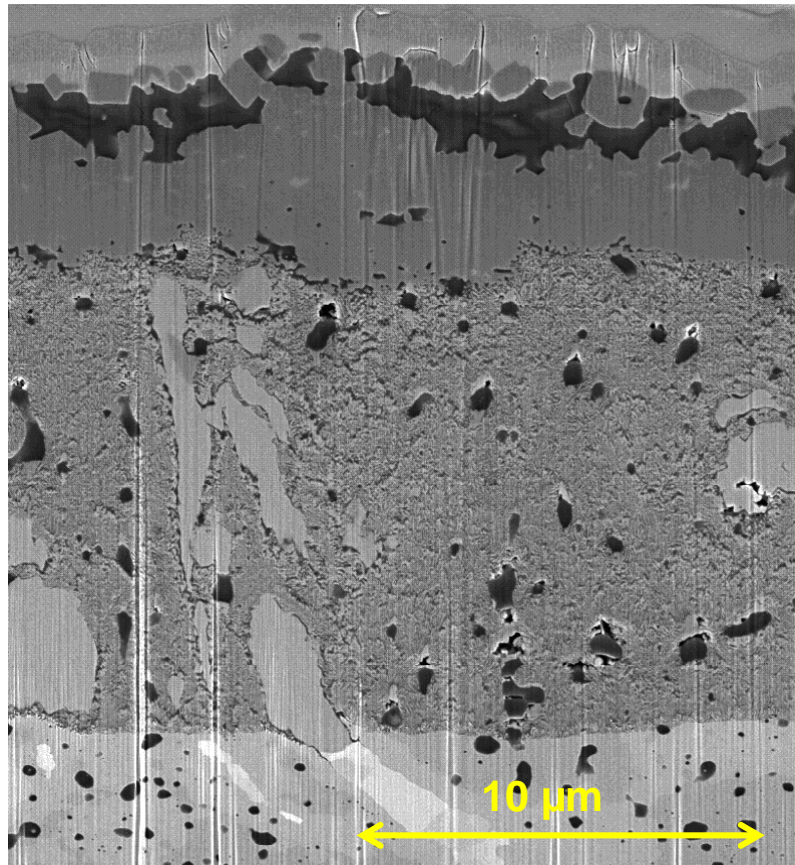
Comparison of parabolic rate constants

- strong passivation at 800°C, comparable to quaternary alloy layers

Oxidation tests: W Si10 Cr10 at 1000 °C, 3h



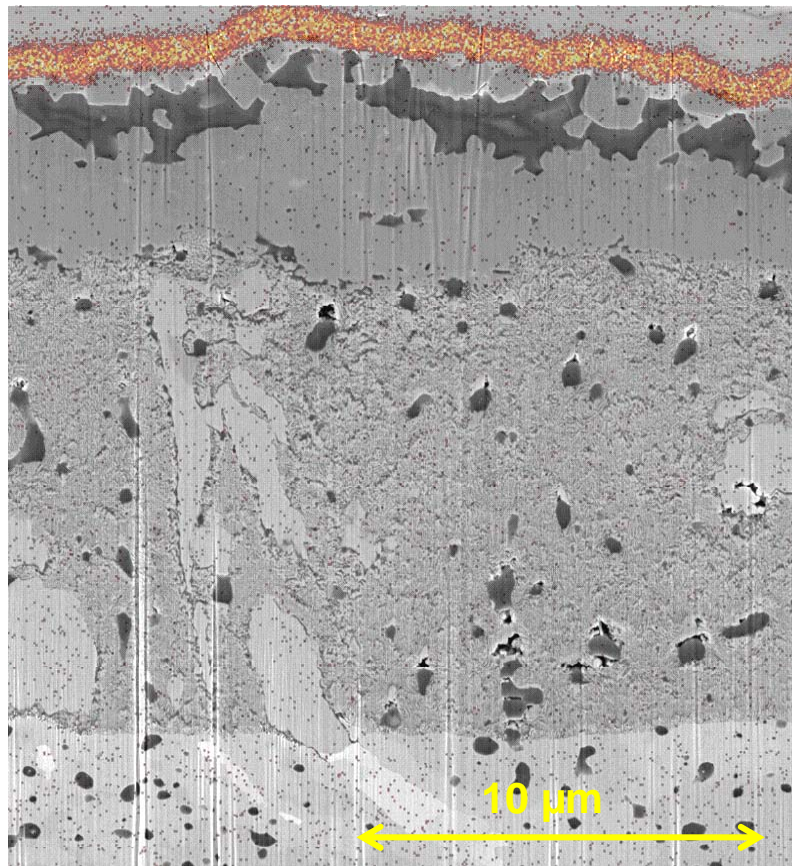
Cross section



Oxidation tests: W Si10 Cr10 at 1000 °C, 3h



Cross section, EDX mapping: Cu

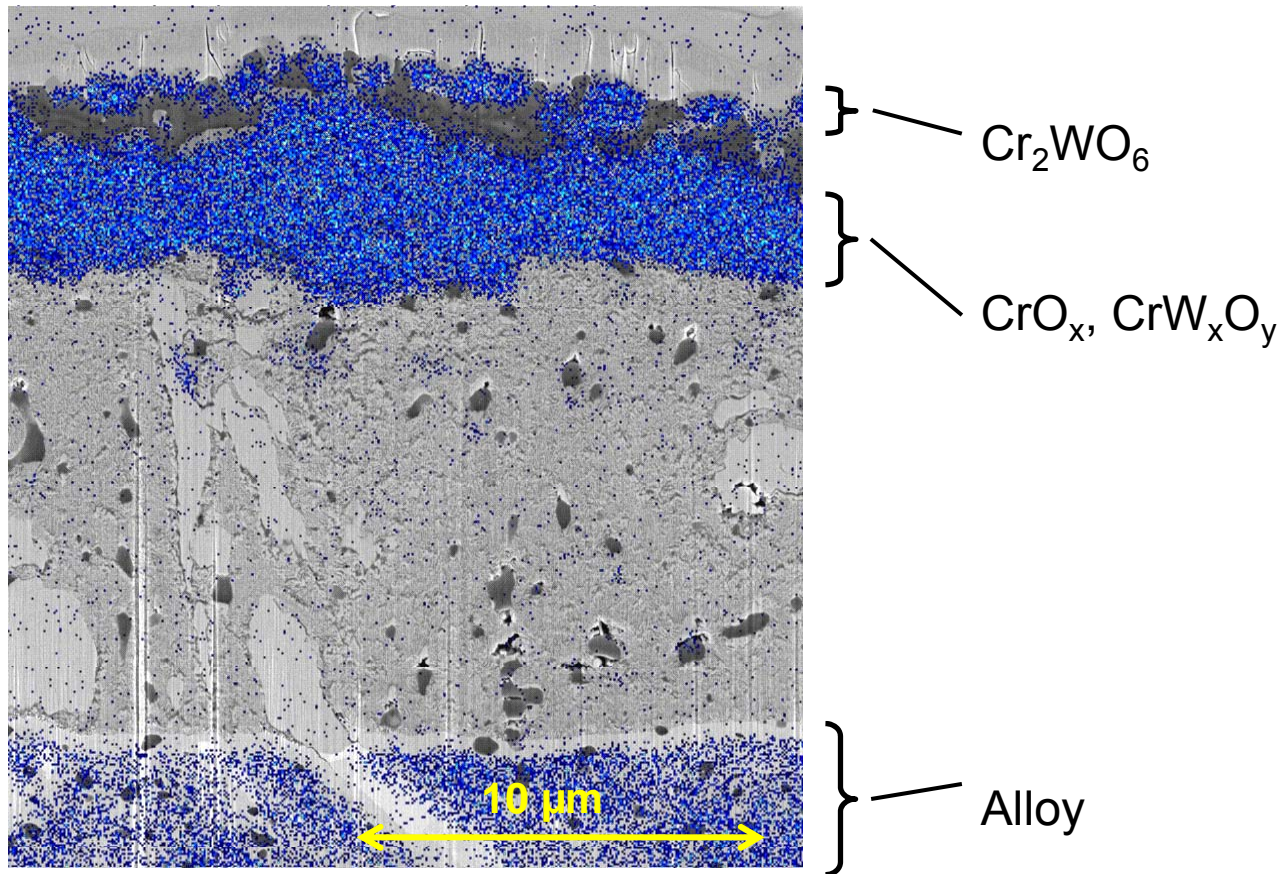


— Cu protection

Oxidation tests: W Si10 Cr10 at 1000 °C, 3h



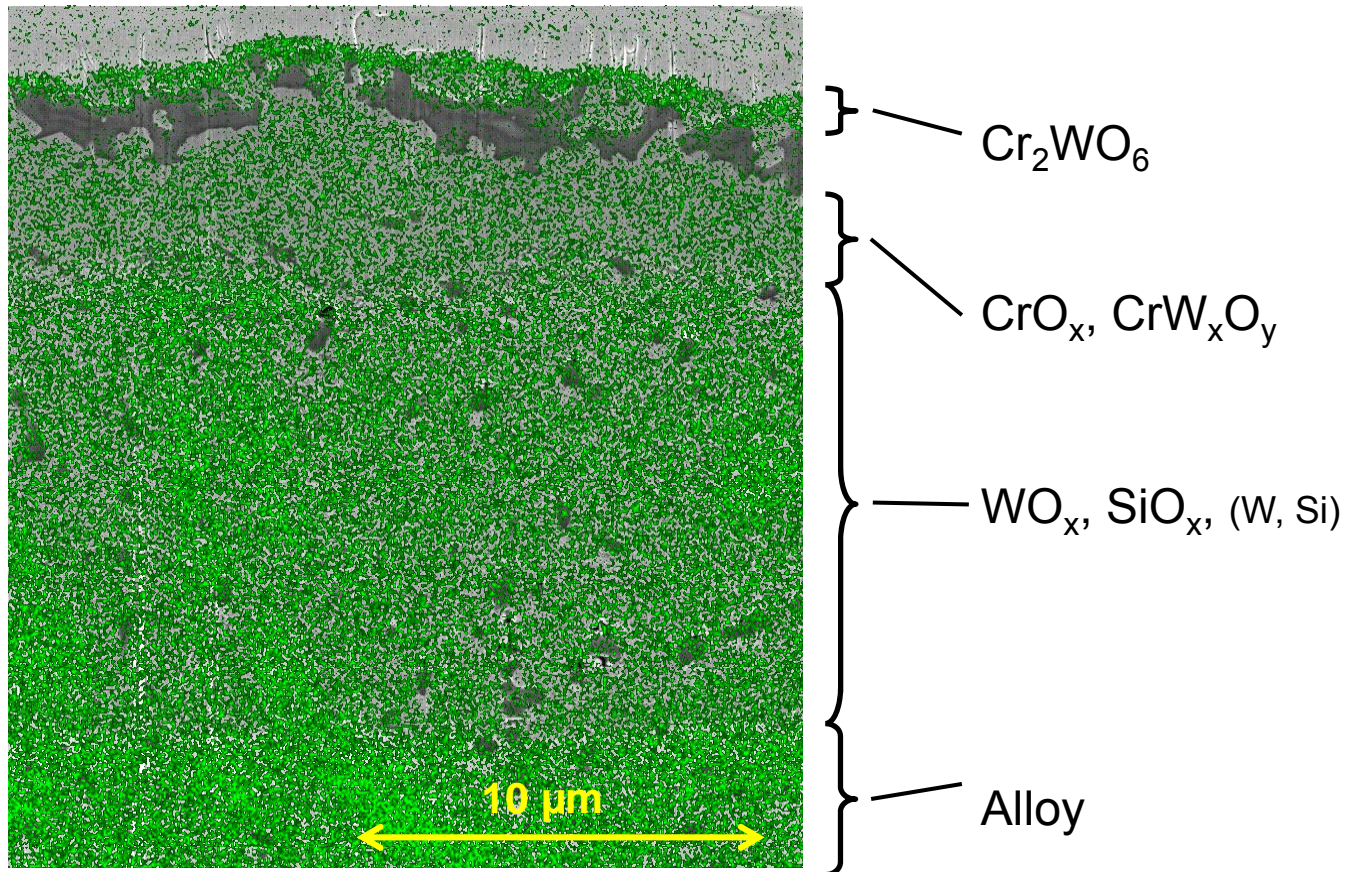
Cross section, EDX mapping: Cr



Oxidation tests: W Si10 Cr10 at 1000 °C, 3h



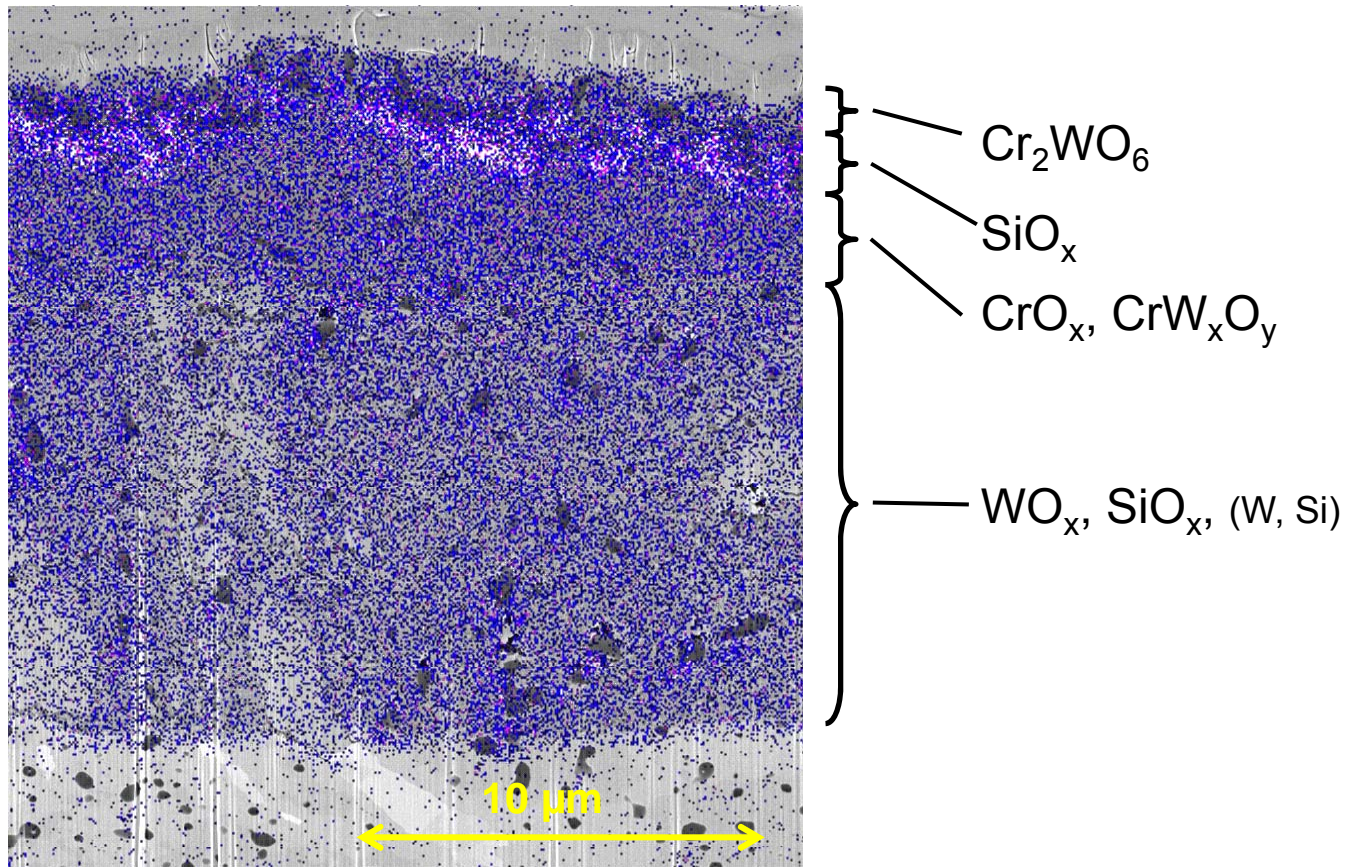
Cross section, EDX mapping: W



Oxidation tests: W Si10 Cr10 at 1000 °C, 3h



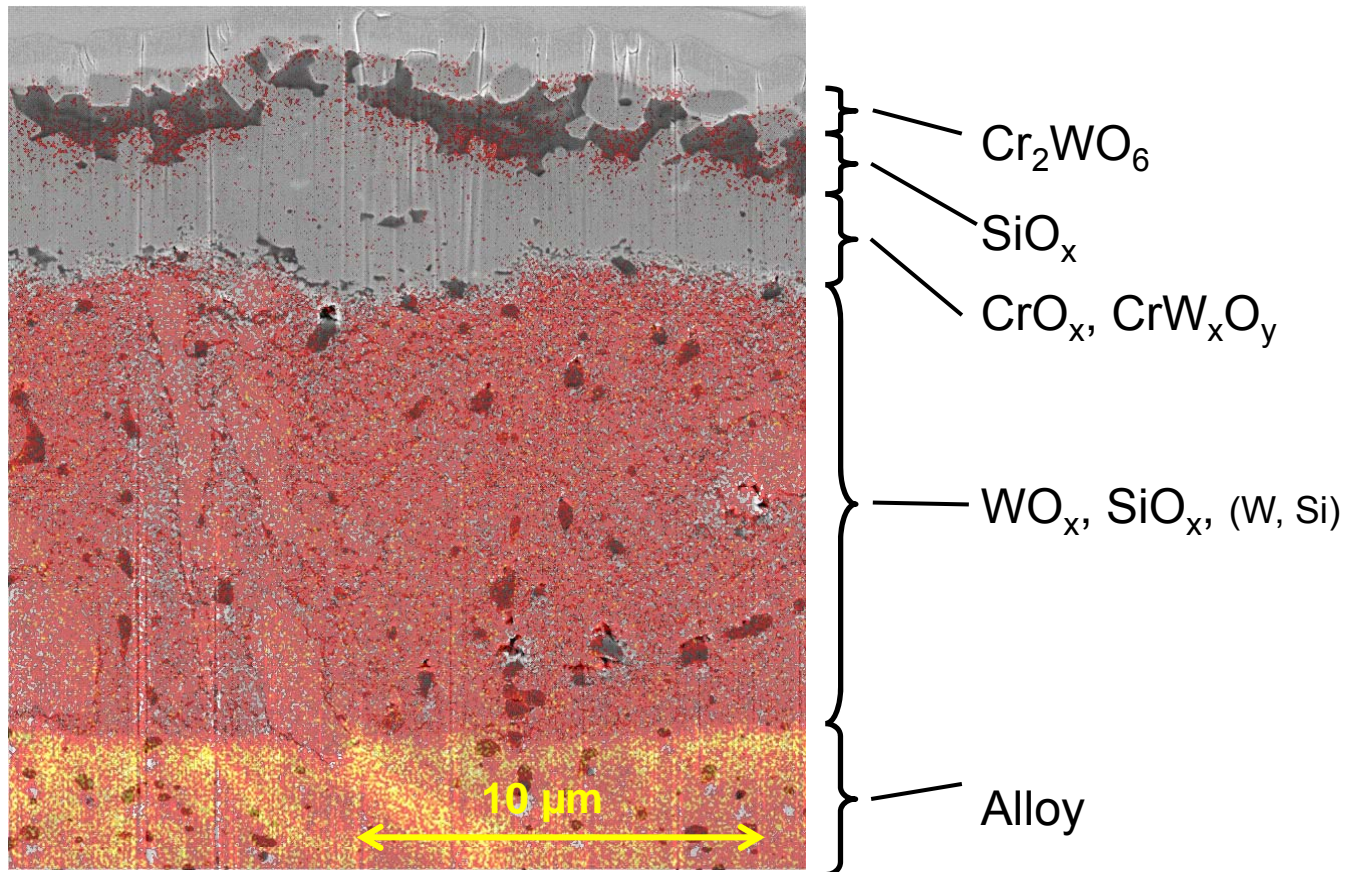
Cross section, EDX mapping: ○



Oxidation tests: W Si10 Cr10 at 1000 °C, 3h



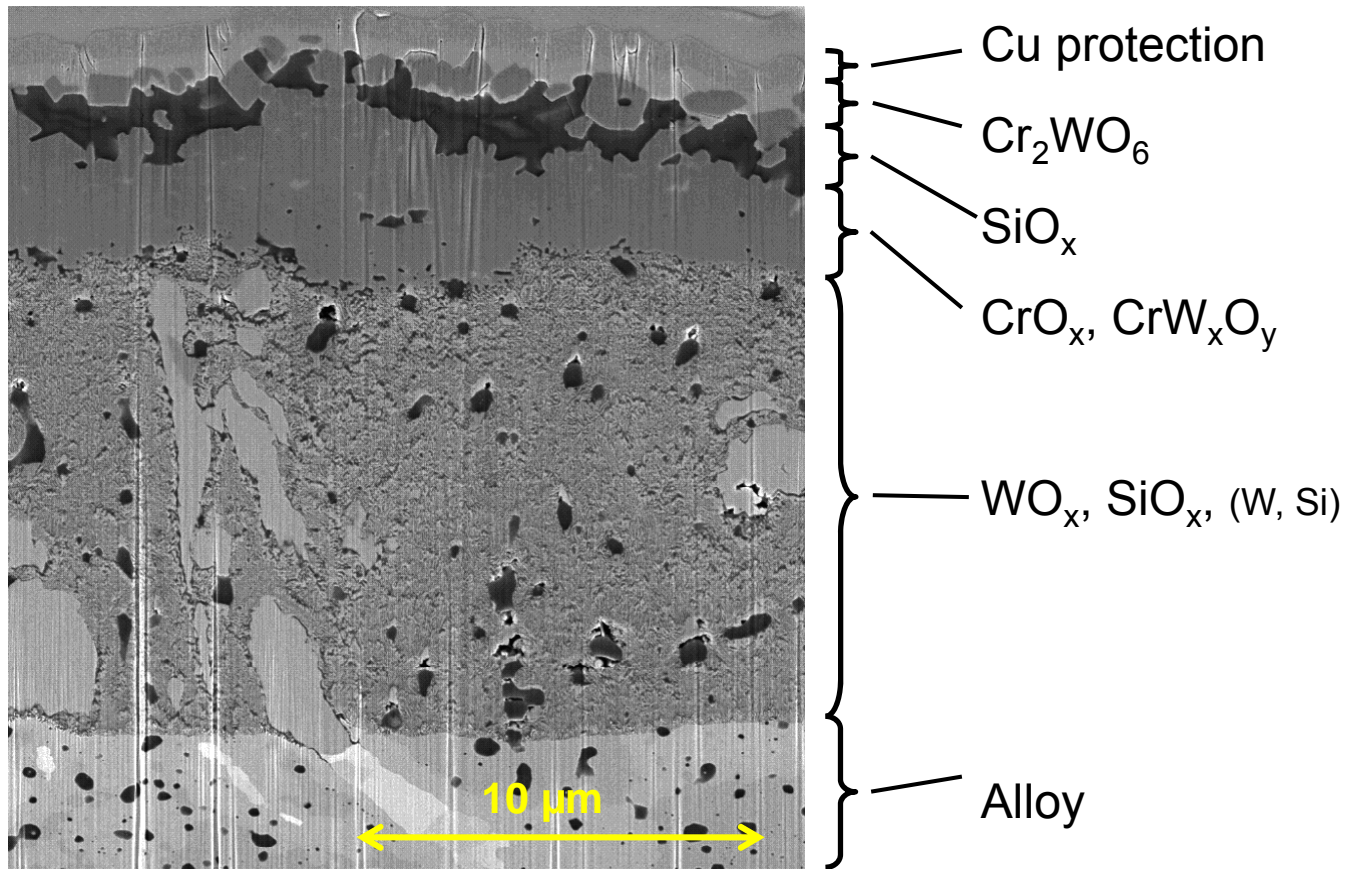
Cross section, EDX mapping: Si (+ W)



Oxidation tests: W Si10 Cr10 at 1000 °C, 3h



Results of EDX and XRD analysis



- W-Cr alloys
- W-Si: hints from XRD
- pure W phase still present in precipitates
- Si-O precipitates
- no visible pores
- oxidation rates promising at 800°C,
CrO_x and Cr₂WO₆ at 1000 °C

Further investigations, ideas:

- optimization (Si-free alloys, increase W fraction in quaternary alloys ...)
 - production and characterization of bulk alloys (IPP in co-operation with CEIT)
 - preferential sputtering with H / D / He ...
 - true surface composition at different annealing states
 - retention and release of hydrogen isotopes
 - comparison of surface layers with bulk alloys (same composition)
 - surface chemical reactions as a plasma-facing material (“material mixing”)
- Promising self-passivating material for a reactor application